

Angular distribution studies on the two-photon ionization of hydrogen-like ions: Relativistic description[‡]

Peter Koval, Stephan Fritzsche and Andrey Surzhykov[†]

Fachbereich Physik, Universität Kassel, Heinrich-Plett Str. 40, D-34132 Kassel, Germany

Abstract. The angular distribution of the emitted electrons, following the two-photon ionization of the hydrogen-like ions, is studied within the framework of second order perturbation theory *and* the Dirac equation. Using a density matrix approach, we have investigated the effects which arise from the polarization of the incoming light as well as from the higher multipoles in the expansion of the electron–photon interaction. For medium- and high- Z ions, in particular, the non-dipole contributions give rise to a significant change in the angular distribution of the emitted electrons, if compared with the electric-dipole approximation. This includes a strong forward emission while, in dipole approximation, the electron emission always occurs symmetric with respect to the plane which is perpendicular to the photon beam. Detailed computations for the dependence of the photoelectron angular distributions on the polarization of the incident light are carried out for the ionization of H, Xe⁵³⁺, and U⁹¹⁺ (hydrogen-like) ions.

1. Introduction

During the last decades, the multi-photon ionization of atoms and ions has been widely studied, both experimentally and theoretically. While, however, the majority of experiments were first of all concerned with the multi-photon ionization of complex atoms, most theoretical investigations instead dealt with the ionization (and excitation) of the much simpler hydrogen-like and helium-like systems. For atomic hydrogen, in contrast, multi-photon experiments have been carried out only recently (Wolff *et al* 1988, Rottke *et al* 1990, Antoine *et al* 1996) because of the former lack of sufficiently intensive (and coherent) light sources in the UV and EUV region. With the recent progress in the setup of intensive light sources in the EUV and x-ray domain, such as the fourth-generation synchrotron facilities or variously proposed free-electron lasers, two- and multi-photon studies on the ionization of inner-shell electrons are now becoming more likely to be carried out in the future, including case studies on medium- Z

[‡] This is the preprint of the original: Peter Koval, Stephan Fritzsche and Andrey Surzhykov, 2004 *J. Phys. B: At. Mol. Opt. Phys.* **37** 375–388.

[†] To whom correspondence should be addressed (surz@physik.uni-kassel.de)

and high- Z *hydrogen-like* ions (Kornberg *et al* 2002). With increasing charge (and intensity of the light), of course, relativistic effects will become important and have been investigated in the past for the two-photon excitation and decay (Goldman and Drake 1981, Szymanowski *et al* 1997, Santos *et al* 2001) as well as ionization (Koval *et al* 2003) of hydrogen-like ions. So far, however, all of these studies were focused on the total (excitation or decay) rates and ionization cross sections while, to the best of our knowledge, no attempts have been made to analyze the effects of relativity on *angular* resolved studies.

In this contribution, we explore the angular distribution of the electrons following the two-photon ionization of hydrogen-like ions. Second-order perturbation theory, based on Dirac's equation, is applied to calculate the two-photon amplitudes including the full (relativistic) electron–photon interaction. The angular distribution of the photoelectrons are then derived by means of the density matrix theory which has been found appropriate for most collision and ionization processes and, in particular, for angular-dependent studies (Laplanche *et al* 1986). Since, however, the basic concepts of the density matrix theory has been presented elsewhere at various places (Blum 1981, Balashov *et al* 2000), we will restrict ourselves to rather a short account of this theory in Subsection 2.1. Apart from a few basic relations, here we only show how the angular distribution of the electrons can be traced back to the two-photon transition amplitudes. The evaluation of these amplitudes in second-order perturbation theory and by means of Coulomb–Green's functions are discussed later in Subsections 2.2 and 2.3, and including the full decomposition of the photon field in terms of its multipole components in Subsection 2.4. Using such a decomposition, we have calculated the electron angular distributions for the two-photon ionization of the $1s$ ground state of hydrogen (H) as well as hydrogen-like xenon (Xe^{53+}) and uranium (U^{91+}). By comparing the angular distributions for different nuclear charges Z , we were able to analyze both, the effects of the polarization of the — incoming — light and the contributions from higher (i.e. non-dipole) multipoles in the decomposition of the electron–photon interaction. These results are displayed in Section 3 and clearly show that, with increasing charge Z , the higher multipole components lead to a strong emission in forward direction (i.e. parallel to the propagation of the light), while the electric-dipole approximation alone gives rise to a symmetric electron emission around the polar angle $\theta \approx 90^\circ$, similar as obtained by nonrelativistic computations (Zernik 1964, Lambropoulos 1972, Arnous *et al* 1973). Finally, a brief summary on the two-photon ionization of medium and high- Z ions is given in Section 4.

2. Theory

2.1. Density matrix approach

Within the density matrix theory, the state of a physical system is described in terms of so-called *statistical* (or *density*) operators (Fano 1957). These operators can be consi-

dered to represent, for instance, an ensemble of systems which are — altogether — in either a *pure* quantum state or in a *mixture* of different states with any degree of coherence. Then, the basic idea of the density matrix formalism is to *accompany* such an ensemble through the collision process, starting from a well defined 'initial' state and by passing through one or, possibly, several intermediate states until the 'final' state of the collision process is attained.

In the two-photon ionization of hydrogen-like ions, the 'initial' state of the (combined) system 'ion *plus* photons' is given by the bound electron $|n_b j_b \mu_b\rangle$ and the two incoming photons, if we assume a zero nuclear spin $I = 0$. For the sake of simplicity, we also restrict our treatment to the case that both photons will have *equal* momentum: $\mathbf{k}_1 = \mathbf{k}_2 = \mathbf{k}$, while the spin states of the photons may still differ from each other and are characterized in terms of the *helicity* parameters $\lambda_1, \lambda_2 = \pm 1$ (i.e. by means of their spin projections onto the direction of propagation \mathbf{k}). Of course, the case of equal photon momenta \mathbf{k} correspond to the most frequent experimental setup of the two-photon ionization of atoms and ions using, for instance, lasers or synchrotron radiation sources. With these assumptions in mind, the initial spin state of the overall system is determined by the direct product of the statistical operators of the ion and the two incident photons

$$\hat{\rho}_i = \hat{\rho}_b \otimes \hat{\rho}_\gamma \otimes \hat{\rho}_\gamma \quad (1)$$

or, explicitly, in a representation of the density matrix in terms of the individual momenta by

$$\begin{aligned} &\langle n_b j_b \mu_b, \mathbf{k} \lambda_1, \mathbf{k} \lambda_2 | \hat{\rho}_i | n_b j_b \mu'_b, \mathbf{k} \lambda'_1, \mathbf{k} \lambda'_2 \rangle \\ &= \langle n_b j_b \mu_b | \hat{\rho}_b | n_b j_b \mu'_b \rangle \langle \mathbf{k} \lambda_1 | \hat{\rho}_\gamma | \mathbf{k} \lambda'_1 \rangle \langle \mathbf{k} \lambda_2 | \hat{\rho}_\gamma | \mathbf{k} \lambda'_2 \rangle . \end{aligned} \quad (2)$$

In the 'final' state of the ionization, after the electron has *left* the nucleus, we just have a free electron with asymptotic momentum \mathbf{p} and spin projection m_s (as well as the bare residual ion with nuclear charge Z). Therefore, the final spin state is described by the statistical operator of the emitted (free) electron $\hat{\rho}_e$ which, in the framework of the density matrix theory, can be obtained from the initial-state density operator $\hat{\rho}_i$ owing to the relation (Blum 1981, Balashov 2001)

$$\hat{\rho}_f = \hat{\rho}_e = \hat{R} \hat{\rho}_i \hat{R}^\dagger . \quad (3)$$

In this simple relation, \hat{R} is called the transition operator and must describe the interaction of the electron with the (two photons of the) radiation field. Of course, the particular form of the transition operator \hat{R} depends on the framework in which we describe the coupling of the radiation field to the atom. As appropriate for high- Z ions, below we will always refer to a *relativistic* treatment of the electron–photon interaction, based on Dirac's equation and the *minimal coupling* of the radiation field (Berestetskii *et al* 1971).

Instead of applying Eq. (3), in practise, it is often more convenient to rewrite the statistical operators in a matrix representation. Using, for example, the initial spin

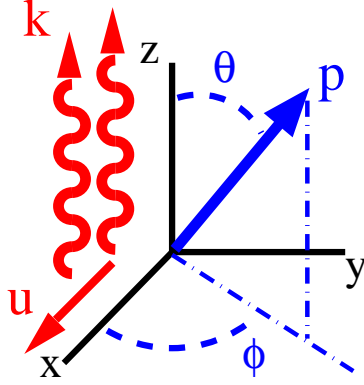


Figure 1. Geometry of the two-photon ionization. The photoelectron is emitted along the unit vector $\hat{\mathbf{p}} = (\theta, \phi)$ where θ is the (polar) angle between the incident photon momenta \mathbf{k} (chosen as the z -axis) and the electron momentum \mathbf{p} . Moreover, the (azimuthal) angle ϕ defines the angle of \mathbf{p} with respect to the x - z plane which, in the case of linearly-polarized light, contains the polarization vector \mathbf{u} .

density matrix (2), we easily obtain the density matrix of the (finally) emitted electron by

$$\langle \mathbf{p} m_s | \hat{\rho}_e | \mathbf{p} m'_s \rangle = \sum_{\mu_b \mu'_b} \sum_{\lambda_1 \lambda'_1 \lambda_2 \lambda'_2} \langle n_b j_b \mu_b | \hat{\rho}_b | n_b j_b \mu'_b \rangle \langle \mathbf{k} \lambda_1 | \hat{\rho}_\gamma | \mathbf{k} \lambda'_1 \rangle \langle \mathbf{k} \lambda_2 | \hat{\rho}_\gamma | \mathbf{k} \lambda'_2 \rangle \times M_{b\mathbf{p}}(m_s, \mu_b, \lambda_1, \lambda_2) M_{b\mathbf{p}}^*(m'_s, \mu'_b, \lambda'_1, \lambda'_2), \quad (4)$$

where used is made of the abbreviation

$$M_{b\mathbf{p}}(m_s, \mu_b, \lambda_1, \lambda_2) = \left\langle \mathbf{p} m_s \left| \hat{R} \right| \mathbf{k} \lambda_1, \mathbf{k} \lambda_2, n_b j_b \mu_b \right\rangle \quad (5)$$

in order to represent the transition amplitudes for the two-photon ionization. The final-state density matrix (4) still contains the *complete* information about the ionization process (i.e. the properties of the bare ion *and* the electron) and, thus, can be used to derive all the observable properties of the photoelectrons. Obviously, however, the outcome of some considered experiment will depend on the particular setup and the capability of the detectors for *resolving* the individual properties of the particles. In the density matrix theory, this setup of the experiment is typically described in terms of a (so-called) *detector operator* \hat{P} which characterizes the detector system as a whole. In fact, this detector operator can be considered to project out all those quantum states of the final-state system which leads to a 'count' at the detectors; in the language of the density matrix, therefore, the probability for an 'event' at the detector is simply given by the trace of the detector operator with the density matrix: $W = \text{Tr}(\hat{P} \hat{\rho})$.

To determine, for instance, the angular distribution of the emitted (photo-) electrons, we may assume a detector operator in a given direction $\hat{p} = (\theta, \phi)$ [cf. Figure 1] which is *insensitive* to the polarization of the electrons

$$\hat{P} = \sum_{m_s} |\mathbf{p} m_s\rangle \langle \mathbf{p} m_s|, \quad (6)$$

i.e. a projection operator along \mathbf{p} and including a summation over the spin state m_s of the electrons. From this operator, and by taking the trace over the product ($\hat{P}\hat{\rho}$) with the final-state density matrix (4), we obtain immediately the electron angular distribution in the form

$$W(\hat{p}) = \text{Tr}(\hat{P}\hat{\rho}_f) = \frac{1}{2j_b + 1} \sum_{\mu_b m_s} \sum_{\lambda_1 \lambda'_1 \lambda_2 \lambda'_2} \langle \mathbf{k}\lambda_1 | \hat{\rho}_\gamma | \mathbf{k}\lambda'_1 \rangle \langle \mathbf{k}\lambda_2 | \hat{\rho}_\gamma | \mathbf{k}\lambda'_2 \rangle \\ \times M_{b\mathbf{p}}(m_s, \mu_b, \lambda_1, \lambda_2) M_{b\mathbf{p}}^*(m_s, \mu_b, \lambda'_1, \lambda'_2) \quad (7)$$

where, for the sake of simplicity, we have assumed that the hydrogen-like ion is initially unpolarized. Apart from this additional assumption, however, Eq. (7) still represents the general form of the electron angular distribution for the process of the two-photon ionization of hydrogen-like ions. As seen from this equation, the emission of the photoelectron will depend on the spin state of the incident photons, defined by the photon density matrices $\langle \mathbf{k}\lambda | \hat{\rho}_\gamma | \mathbf{k}\lambda' \rangle$. For any further evaluation of this distribution function, therefore, we shall first specify these density matrices or, in other words, the polarization of the incoming light. For example, if both photons are *unpolarized*, the (two) photon density matrices simply reduce to a constant $1/2$, $\langle \mathbf{k}\lambda | \hat{\rho}_\gamma | \mathbf{k}\lambda' \rangle = \delta_{\lambda\lambda'}/2$ [cf. Appendix, Eq. A.2] and leads us to the well-known angular distribution

$$W^{\text{unp}}(\hat{p}) = \frac{1}{4(2j_b + 1)} \sum_{\mu_b m_s} \sum_{\lambda_1 \lambda_2} |M_{b\mathbf{p}}(m_s, \mu_b, \lambda_1, \lambda_2)|^2. \quad (8)$$

For many (modern) light sources such as lasers or synchrotron radiation, it is not very practical to consider only *unpolarized* light from the very beginning. In general, instead, the angular distribution of the emitted electrons will depend both on the *type* as well as the *degree* of the polarization of the incident light. For *circularly* polarized light with degree P_C , for instance, the photon density matrix from Eq. (7) becomes $\langle \mathbf{k}\lambda | \hat{\rho}_\gamma | \mathbf{k}\lambda' \rangle = (1 + \lambda P_C) \delta_{\lambda\lambda'}/2$ and, hence, give rise to the angular distribution

$$W_{P_C}^{\text{circ}}(\hat{p}) = \frac{1}{4(2j_b + 1)} \sum_{\mu_b m_s \lambda_1 \lambda_2} (1 + \lambda_1 P_C) (1 + \lambda_2 P_C) |M_{b\mathbf{p}}(m_s, \mu_b, \lambda_1, \lambda_2)|^2, \quad (9)$$

while, for *linearly* polarized light along the x -axis and with a polarization degree P_L , the photon density matrix is $\langle \mathbf{k}\lambda | \hat{\rho}_\gamma | \mathbf{k}\lambda' \rangle = \delta_{\lambda\lambda'}/2 + (1 - \delta_{\lambda\lambda'})P_L/2$. If we evaluate Eq. (7) again with this latter density matrix, we obtain the angular distribution

$$W_{P_L}^{\text{lin}}(\hat{p}) = \frac{1}{4(2j_b + 1)} \sum_{\mu_b m_s} \left((1 - P_L)^2 \sum_{\lambda_1 \lambda_2} |M_{b\mathbf{p}}(m_s, \mu_b, \lambda_1, \lambda_2)|^2 \right. \\ \left. P_L^2 \left| \sum_{\lambda_1 \lambda_2} M_{b\mathbf{p}}(m_s, \mu_b, \lambda_1, \lambda_2) \right|^2 \right) \quad (10)$$

for the electrons as emitted in the two-photon ionization of hydrogen-like ions with linearly polarized light.

2.2. Two-photon transition amplitude in second-order perturbation theory

For any further analysis of the electron angular distributions, following the two-photon ionization of a hydrogen-like ion, we need to calculate the transition amplitude $M_{b\mathbf{p}}(m_s, \mu_b, \lambda_1, \lambda_2)$ as seen from Eqs. (8)–(10). This amplitude describes a *bound-free* transition of the electron under the (simultaneous) absorption of two photons. For a moderate intensity of the photon field, of course, this amplitude is most simply calculated by means of second-order perturbation theory (Laplanche *et al* 1976)

$$M_{b\mathbf{p}}(m_s, \mu_b, \lambda_1, \lambda_2) = \sum_{\nu}^f \frac{\langle \psi_{\mathbf{p}m_s} | \alpha \mathbf{u}_{\lambda_1} e^{i\mathbf{k}r} | \psi_{\nu} \rangle \langle \psi_{\nu} | \alpha \mathbf{u}_{\lambda_2} e^{i\mathbf{k}r} | \psi_{n_b j_b \mu_b} \rangle}{E_{\nu} - E_b - E_{\gamma}}, \quad (11)$$

where the transition operator $\alpha \mathbf{u}_{\lambda} e^{i\mathbf{k}r}$ describes the (relativistic) electron–photon interaction, the unit vector \mathbf{u}_{λ} the polarization of the photons, and where the summation runs over the complete one-particle spectrum. From the energy conservation, moreover, it follows immediately that the energies of the initial bound state, E_b , and the final continuum state, E_f , are related to each other by $E_f = E_b + 2E_{\gamma}$, owing to the energy of the incoming photons, $E_{\gamma} = \hbar ck$. Although known for a long time, the *relativistic* form of the transition amplitude (11) has been used only recently in studying multi-photon ionization processes and, in particular, in order to calculate the total ionization cross sections along the hydrogen isoelectronic sequence (Koval *et al* 2003). In such a relativistic description of the transition amplitude (11), the initial state $\psi_{n_b j_b \mu_b}(\mathbf{r}) = \langle \mathbf{r} | n_b j_b \mu_b \rangle$ and the final state $\psi_{\mathbf{p}m_s}(\mathbf{r}) = \langle \mathbf{r} | \mathbf{p}m_s \rangle$ are the (analytically) well-known solutions of the Dirac Hamiltonian for a bound and continuum electron, respectively (Berestetskii *et al* 1971).

As seen from Eq. (11), the evaluation of the transition amplitude requires a summation over the *discrete* (bound) states as well as an integration over the *continuum* of the Dirac Hamiltonian, (ψ_{ν}, E_{ν}) . In fact, such a ‘summation’ over the complete spectrum is difficult to carry out explicitly since, in particular the integration over the continuum requires the calculation of *free-free* transitions. In the past, therefore, this summation has often been restricted to some small — *discrete* — basis, assuming that the contribution from the continuum is negligible. In practise, however, such a limitation seems justified only to estimate the behaviour of the cross sections near the resonances where the ion is rather likely excited by the first photon into some — real — intermediate state of the ion from which it is later ionized by means of a second photon. In the *non-resonant* region of the photon energies, in contrast, the integration over the continuum may give rise to a rather remarkable contribution to the total cross section and, hence, has to be carried out. Apart from a *direct summation* over the continuum states, however, it is often more favorable to apply Green’s functions, at least if these functions can be generated efficiently. For hydrogen-like ions, for example, such Green’s functions are known analytically, both in the nonrelativistic as well as relativistic theory (Swainson and Drake 1991).

2.3. Green's function approach

As usual, Green's functions are defined as solutions to some inhomogeneous (differential) equation

$$(E - \hat{H}) G_E(\mathbf{r}, \mathbf{r}') = \delta(\mathbf{r} - \mathbf{r}') \quad (12)$$

where, in our present investigation, \hat{H} refers the Dirac Hamiltonian and E denotes the energy of the atom or ion. For realistic systems, of course, such Green's functions are not easy to obtain, even if only *approximate* solutions are needed. However, a formal solution is given by (Morse and Feshbach 1953)

$$G_E(\mathbf{r}, \mathbf{r}') = \sum_{\nu}^{\dagger} \frac{|\psi_{\nu}(\mathbf{r})\rangle \langle \psi_{\nu}(\mathbf{r}')|}{E_{\nu} - E}, \quad (13)$$

including a summation (integration) over the complete spectrum (of \hat{H}) as discussed in the previous section. In the two-photon transition amplitude (11), therefore, we may simply replace this summation by the corresponding Green's function

$$M_{\mathbf{b}\mathbf{p}}(m_s, \mu_b, \lambda_1, \lambda_2) = \left\langle \psi_{\mathbf{p}m_s}(\mathbf{r}) \left| \alpha \mathbf{u}_{\lambda_1} e^{i\mathbf{k}\mathbf{r}} G_{E_b+E_{\gamma}}(\mathbf{r}, \mathbf{r}') \alpha \mathbf{u}_{\lambda_2} e^{i\mathbf{k}\mathbf{r}'} \right| \psi_{n_b\kappa_b\mu_b}(\mathbf{r}') \right\rangle. \quad (14)$$

For hydrogen-like ions, the Coulomb–Green's functions from Eq. (12) are known analytically today in terms of (various) special functions from mathematical physics and, in particular, in terms of the confluent hypergeometric function ${}_1F_1(a, b, z)$. Here, we will not display these functions explicitly but refer the reader instead to the literature (Swainson and Drake 1991, Koval and Fritzsche 2003). For the further evaluation of the transition amplitudes (14) let us note only that, also for the one-particle Dirac Hamiltonian, the Coulomb–Green's function can be decomposed into a radial and an angular part

$$G_E(\mathbf{r}, \mathbf{r}') = \frac{1}{rr'} \sum_{\kappa m} \begin{pmatrix} g_{E\kappa}^{LL}(r, r') \Omega_{\kappa m}(\hat{r}) \Omega_{\kappa m}^{\dagger}(\hat{r}') & -i g_{E\kappa}^{LS}(r, r') \Omega_{\kappa m}(\hat{r}) \Omega_{-\kappa m}^{\dagger}(\hat{r}') \\ i g_{E\kappa}^{SL}(r, r') \Omega_{-\kappa m}(\hat{r}) \Omega_{\kappa m}^{\dagger}(\hat{r}') & g_{E\kappa}^{SS}(r, r') \Omega_{-\kappa m}(\hat{r}) \Omega_{-\kappa m}^{\dagger}(\hat{r}') \end{pmatrix}, \quad (15)$$

where the $\Omega_{\kappa m}(\hat{r})$ denote standard Dirac spinors and where the radial Green's function is given in terms of four components $g_{E\kappa}^{TT'}(r, r')$ with $T = L, S$ referring to the *large* and *small* components of the associated (relativistic) wave functions. The computation of the radial Green's function for hydrogen-like ions has been described and implemented previously into the GREENS library (Koval and Fritzsche 2003); this code has been used also for the computation of all transition amplitudes and (angle-differential) cross sections as shown and discussed below.

2.4. Exact relativistic formulation of the two-photon amplitude

Eq. (14) displays the two-photon transition amplitude in terms of the (relativistic) wave and Green's functions of hydrogen-like ions. For the further evaluation of this amplitude, we need to decompose both, the photon as well as the free-electron wave functions into partial waves in order to make later use of the techniques of Racah's algebra. As discussed previously for the capture of electrons by bare, high-Z ions (Surzhykov

et al 2002), we first have to decide about a proper quantization axis (z -axis) for this decomposition, depending — of course — on the particular process under consideration. For the photoionization of atoms, the only really *preferred* direction of the overall system is given by the photon momenta $\mathbf{k}_1 = \mathbf{k}_2 = \mathbf{k}$ which we adopt as the quantization axis below. Then, the multipole expansion of the radiation field reads as

$$\mathbf{u}_\lambda e^{i\mathbf{k}\mathbf{r}} = \mathbf{u}_\lambda e^{ikz} = \sqrt{2\pi} \sum_{L=1}^{\infty} i^L [L]^{1/2} \left(\mathbf{A}_{L\lambda}^{(m)} + i\lambda \mathbf{A}_{L\lambda}^{(e)} \right), \quad (16)$$

where $[L] = (2L + 1)$ and the standard notation $\mathbf{A}_{LM}^{(e,m)}$ is used for the electric and magnetic multipole fields, respectively. Each of these multipoles can be expressed in terms of the spherical Bessel functions $j_L(kr)$ and the vector spherical harmonics $\mathbf{T}_{L,\Lambda}^M$ of rank L as (Rose 1957):

$$\begin{aligned} \mathbf{A}_{LM}^{(m)} &= j_L(kr) \mathbf{T}_{L,L}^M, \\ \mathbf{A}_{LM}^{(e)} &= j_{L-1}(kr) \sqrt{\frac{L+1}{2L+1}} \mathbf{T}_{L,L-1}^M - j_{L+1}(kr) \sqrt{\frac{L}{2L+1}} \mathbf{T}_{L,L+1}^M. \end{aligned} \quad (17)$$

Using the expressions (16) and (17) for the photon field, we can rewrite the two-photon transition amplitude (14) in terms of its *electric-magnetic* components

$$\begin{aligned} M_{b\mathbf{p}}(m_s, \mu_b, \lambda_1, \lambda_2) &= 2\pi \sum_{L,L'=1}^{\infty} \sum_{\Lambda\Lambda'} i^{L+L'} [L, L']^{1/2} \xi_{\Lambda L}^{\lambda_1} \xi_{\Lambda' L'}^{\lambda_2} \\ &\times \langle \psi_{\mathbf{p}m_s} | \alpha j_\Lambda(kr) \mathbf{T}_{L,\Lambda}^{\lambda_1} G_{E_b+E_\gamma}(\mathbf{r}, \mathbf{r}') \alpha j_{\Lambda'}(kr') \mathbf{T}_{L',\Lambda'}^{\lambda_2} | \psi_{n_b\kappa_b\mu_b} \rangle, \end{aligned} \quad (18)$$

where the coefficients $\xi_{L\Lambda}^\lambda$ are defined as

$$\xi_{L\Lambda}^\lambda = \begin{cases} 1 & \text{if } \Lambda = L \\ i\lambda \sqrt{\frac{L+1}{2L+1}} & \text{if } \Lambda = L - 1 \\ -i\lambda \sqrt{\frac{L}{2L+1}} & \text{if } \Lambda = L + 1 \end{cases}. \quad (19)$$

As seen from the expansion (18), we can distinguish between different multipole components such as E1E1, E1M1, E1E2, and others owing to the symmetries of the two vector spherical harmonics, i.e. due to the particular combination of the summation indices L, L', Λ, Λ' in this expansion. In the second line of (18), however, the — electro-magnetic — multipole matrix elements still contain the wave function $\psi_{\mathbf{p}m_s}(\mathbf{r})$ of the free electron with well-defined asymptotic momentum \mathbf{p} . In another expansion, therefore, we have to decompose it into partial waves to allow for a further simplification of the two-photon transition amplitude (18). Again, also the expansion of the free-electron wave will depend on the choice of the quantization axis and requires — by using a quantization along the photon momentum — that we have to carry out a rotation of the space part of the electron wavefunction from the z -direction into the \mathbf{p} -direction

$$\begin{aligned} \psi_{\mathbf{p}m_s}(\mathbf{r}) &= 4\pi \sum_{\kappa_f \mu_f} i_{\kappa_f}^{L_f} e^{-i\Delta_{\kappa_f}} \langle l_f^L \mu_f - m_s \ 1/2m_s | j_f \mu_f \rangle \\ &\times Y_{l_f^* \mu_f - m_s}^*(\hat{p}) \begin{pmatrix} g_{E\kappa_f}^L(r) \Omega_{\kappa_f \mu_f}(\hat{n}) \\ i g_{E\kappa_f}^S(r) \Omega_{-\kappa_f \mu_f}(\hat{n}) \end{pmatrix}, \end{aligned} \quad (20)$$

where the summation runs over all partial waves $\kappa_f = \pm 1, \pm 2, \dots$, i.e. over all possible values of the Dirac angular momentum quantum number $\kappa_f = \pm(j_f + 1/2)$ for $l_f^L = j_f \pm 1/2$. In this notation, the (nonrelativistic angular) momentum l_f^L represents the parity of the partial waves and Δ_{κ_f} is the Coulomb phase shift. Moreover, as seen from expression (20), the partial waves

$$\psi_{E\kappa m_s}(\mathbf{r}) = \begin{pmatrix} g_{E\kappa_f}^L(r) \Omega_{\kappa_f\mu_f}(\hat{n}) \\ i g_{E\kappa_f}^S(r) \Omega_{-\kappa_f\mu_f}(\hat{n}) \end{pmatrix} \quad (21)$$

separate into a radial and an angular parts, where the two radial functions

$$g_{E\kappa}^L(r) \equiv P_{E\kappa}(r), \quad g_{E\kappa}^S(r) \equiv Q_{E\kappa}(r)$$

are often called the *large* and *small* components and the corresponding angular parts $\Omega_{\kappa_f\mu_f}(\hat{n}) \equiv |l_f^L j_f \mu_f\rangle = \sum_{m_l m_s} \langle l_f^L m_l 1/2 m_s | j_f \mu_f \rangle Y_{l_f^L m_l}(\hat{n}) \chi_{1/2 m_s}$ and $\Omega_{-\kappa_f\mu_f}(\hat{n}) \equiv |l_f^S j_f \mu_f\rangle = \sum_{m_l m_s} \langle l_f^S m_l 1/2 m_s | j_f \mu_f \rangle Y_{l_f^S m_l}(\hat{n}) \chi_{1/2 m_s}$ are the standard Dirac spin-angular functions.

Using the partial-wave decomposition (21) for the free-electron wave function and a similar expansion (15) for the Green's functions, we now can carry out the angular integration in the transition amplitude (18) analytically

$$\begin{aligned} M_b(m_s, \mu_b, \lambda_1, \lambda_2) &= 8\pi^2 \sum_{L\Lambda L'\Lambda'} \sum_{\kappa_f\mu_f} \sum_{\kappa m T T'} i^{L+L'} i^{-l_f^L} P^T P^{T'} e^{i\Delta_{\kappa_f}} \\ &\quad \times [L, L']^{1/2} \xi_{L\Lambda}^{\lambda_1} \xi_{L'\Lambda'}^{\lambda_2} \langle l_f^L \mu_f - m_s 1/2 m_s | j_f \mu_f \rangle \\ &\quad \times \langle \kappa_f l_f^{\overline{T}} \mu_f | \sigma \mathbf{T}_{L\Lambda}^{\lambda_1} | \kappa l^T m \rangle \langle \kappa l^{T'} m | \sigma \mathbf{T}_{L'\Lambda'}^{\lambda_2} | \kappa_b l_b^{\overline{T'}} \mu_b \rangle \\ &\quad \times U_{\Lambda\Lambda'}^{TT'}(\kappa_f, \kappa, \kappa_b) Y_{l_f^L \mu_f - m_s}(\hat{n}) \end{aligned} \quad (22)$$

where, apart from the Clebsch–Gordan coefficient $\langle l_f^L \mu_f - m_s 1/2 m_s | j_f \mu_f \rangle$ and some constant factors, the angular part of the amplitude is given in terms of the matrix elements of the rank L spherical tensor $\sigma \mathbf{T}_{L\Lambda}^{\lambda_1} = [Y_\Lambda \otimes \sigma]_L^M$. These matrix elements can be simplified to (Balashov *et al* 2000)

$$\begin{aligned} \langle \kappa_b l_b^{\overline{T}} \mu_b | \sigma \mathbf{T}_{L\Lambda}^M | \kappa_a l_a^{T'} \mu_a \rangle &= \sqrt{\frac{3}{2\pi}} [j_a, L, \Lambda, l_b^{T'}]^{1/2} \langle j_a \mu_a LM | j_b \mu_b \rangle \\ &\quad \times \langle l_b^{\overline{T}} 0, \Lambda 0 | l_a^{T'} 0 \rangle \begin{Bmatrix} l_b^{\overline{T}} & 1/2 & j_b \\ \Lambda & 1 & L \\ l_a^{T'} & 1/2 & j_a \end{Bmatrix}, \end{aligned} \quad (23)$$

by using a proper decomposition in terms of the orbital and spin subspaces. The radial part of the transition amplitude (18) is contained in (22) in the (two-dimensional) integrals

$$U_{\Lambda\Lambda'}^{TT'}(\kappa_f, \kappa, \kappa_b) = \int g_{E_f\kappa_f}^{\overline{T}}(r) j_\Lambda(kr) g_{E_b+E_\gamma\kappa}^{TT'}(r, r') j_{\Lambda'}(kr') g_{n_b\kappa_b}^{\overline{T'}}(r') dr dr', \quad (24)$$

which combines the various (large and small) components of the bound state, the Green's function as well as from the free-electron wave. In this notation, again, $T = L, S$ and

a superscript \bar{T} refers to the conjugate of T , i.e. $\bar{T} = L$ for $T = S$ and *vice versa*. In contrast to the angular integrals (23), the radial integrals (24) have to be computed numerically. In the present work, all the required integrals for the two-photon transition amplitudes (22) are calculated by using the GREENS (Koval and Fritzsche, 2003) and RACAH (Fritzsche *et al* 2001) programs.

2.5. Electric dipole approximation

The transition amplitude (22) still describes the full interaction between the electron and photon fields. With the explicit summation over all the multipoles of the photon field (16), it includes the so-called *retardation effects* or *non-dipole* contributions. In practise, however, the contributions from the higher multipoles decreases very rapidly with L and may therefore be neglected; in fact, the computation of these contributions also become rather tedious because of difficulties with a stable procedure for the two-dimensional radial integrals (24). In many cases, therefore, it seems justified to restrict the summation in (22) to just the (dominant) *electric dipole* term with $L = 1$ and $\Lambda = L \pm 1$. This 'dipole approximation' is valid if the photon wave length is much larger than the size of the atom, i.e. $ka_0 \ll 1$ where a_0 is the Bohr radius. For the two-photon ionization, this condition is well satisfied for most light ions with, say, $Z < 30$ and for photon energies below of the one-photon ionization threshold.

From the general form (22) of the ionization amplitude, the electric dipole approximation is obtained by taking $L = L' = 1$ and $\Lambda, \Lambda' = 0, 2$ which — owing to the dipole selection rules — then also restricts the summation over κ_f , i.e. the allowed partial waves for the free electron. For the K -shell ionization with (completely) *circularly* polarized light, for instance, the final-state electron can only escape in the $d_{3/2}$ or $d_{5/2}$ states. And, as seen from Eq. (22), the dipole transition amplitude is then indeed defined by the (second-rank) spherical harmonic, $M_{b\mathbf{p}}(m_s, \mu_b, \lambda, \lambda) \propto Y_{2, \mu_b - m_s + 2\lambda}(\hat{p}) \sim \sin^2(\theta)$ which (together with eq. 9) leads us to the well-known angular distribution

$$W^{\text{circ}}(\hat{p}) = c_4 \sin^4 \theta \quad (25)$$

of the photoelectrons (Lambropoulos 1972, Arnous *et al* 1973). As expected from the axial symmetry of the overall system 'ion *plus* photons', the angular distribution (25) only depends on θ but not on the azimuthal angle ϕ . For linearly polarized light, in contrast, a *reaction plane* is naturally defined by the photon momentum \mathbf{k} and the polarization vector \mathbf{u} and, hence, the axial symmetry is broken. For a linear polarization of the incident light, therefore, the angular distribution will depend on both, the polar and azimuthal angle and is given by (Zernik 1964, Lambropoulos 1972)

$$W^{\text{lin}}(\hat{p}) = b_0 + b_2 \sin^2 \theta \cos^2 \phi + b_4 \sin^4 \theta \cos^4 \phi, \quad (26)$$

where the angle $\phi = 0$ corresponds to an electron emission within the reaction plane.

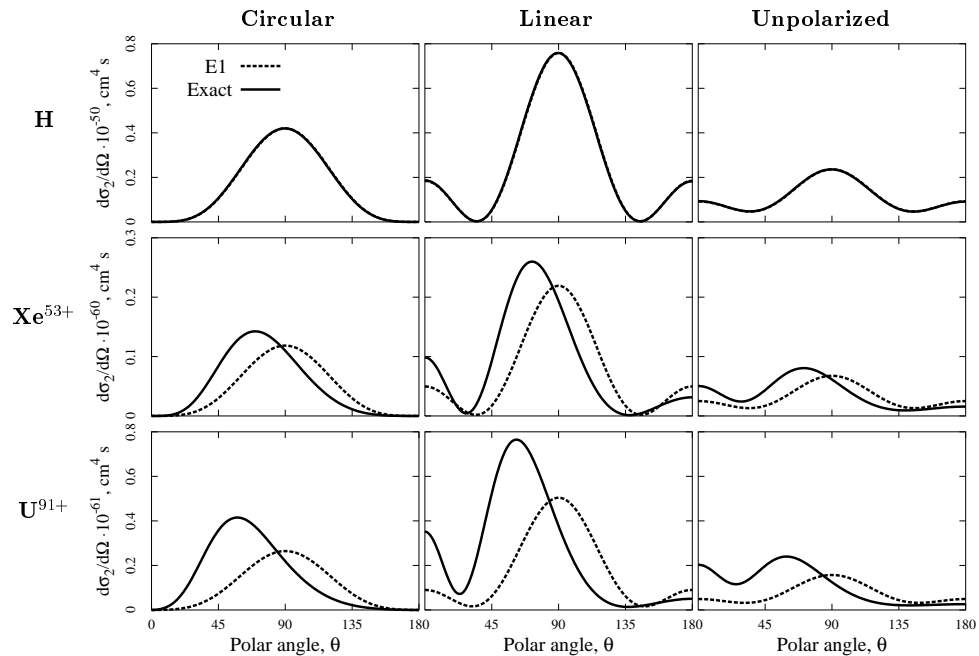


Figure 2. Angular distributions of the emitted electrons in the two-photon K -shell ionization of hydrogen-like ions by means of circularly, linearly and unpolarized light. Results are presented for both, the electric dipole (---) and the relativistic (—) approximations and for a two-photon energy which is 40 % above the (one-photon) ionization threshold.

3. Results and discussion

For the calculation of total two-photon ionization cross sections, the electric dipole approximation was recently found sufficient for most of the hydrogen-like ions, and not just in the low- Z domain (Koval *et al* 2003). Even for high- Z ions, for example, the total cross sections from the dipole approximation do not differ more than about 20 % from those of a full relativistic computation, including the contributions from all the higher multipoles. Larger deviations, however, can be expected for the angular distribution of the emitted electrons which is known to be sensitive to the retardation in the electron-photon interaction. As known, for instance, from the radiative recombination of high- Z ions, a significant change in the angle-differential cross sections may arise from the higher multipoles and may lead to quite sizeable deviations when compared with the dipole approximation (Surzhykov *et al* 2002).

In this contribution, therefore, we have analyzed both, the electric dipole and the exact relativistic treatment from Eq. (22) in order to explore the relativistic and retardation effects on the angular distributions of the electrons. Detailed computations have been carried out, in particular, for the K -shell ionization of (neutral) hydrogen as well as hydrogen-like xenon and uranium. Moreover, to explore the dependence of the relativistic effects on the polarization of the incoming light, three cases of the

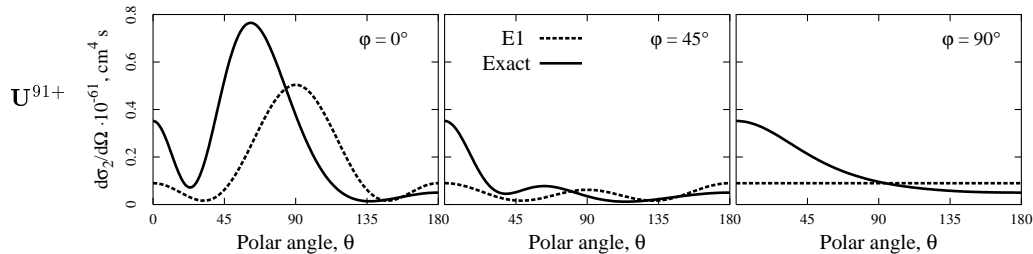


Figure 3. Angular distributions of the electrons emitted in the two-photon K -shell ionization of the hydrogen-like uranium U^{91+} by means of linear polarized light. Distributions are shown for the angles $\phi = 0^\circ$, 45° and 90° with respect to the reaction plane; cf. Figure 1.

polarization are considered: (i) completely circular polarized, (ii) completely linear polarized as well as the case of (iii) unpolarized light. For these three ions and types of polarization, Figure 2 displays the angular distributions of the electrons as obtained by the dipole approximation (---) and the exact relativistic treatment (—). While, for hydrogen, both approximation virtually yields identical results, they start to differ as the nuclear charge Z is increased. Instead of a symmetrical emission with respect to the polar angle $\theta = 90^\circ$, then the emission occurs predominantly into forward direction, an effect which is best seen for hydrogen-like U^{91+} ions. We therefore find, that the *non-dipole* terms give first of all rise to an *asymmetrical* shift in the angular distribution of the electrons which could be observed in experiment. The maxima in the (angle-differential) cross sections, on the other hand, are less affected and deviate, even for hydrogen-like uranium, less than a factor of 2.

In Figure 2, all angular distributions are shown as function of the polar angle θ , i.e. with respect to the incoming photon beam. As discussed above, this dependence of the differential cross sections, $\frac{d\sigma}{d\Omega} = \frac{d\sigma}{d\Omega}(\theta)$, can be the only one for circular and unpolarized light for which the electron emission must be axially symmetric. For linear polarized light, in contrast, the emission of the electrons will depend on both, the polar angle θ and the azimuthal angle ϕ . For this polarization, Figure 2 only displays the angular distributions *within* the reaction plane, i.e. at $\phi = 0^\circ$. To explore, in addition, also the ϕ -dependence of the two-photon ionization by linear polarized light explicitly, Figure 3 shows the corresponding angular distributions $\frac{d^2\sigma}{d\Omega}(\theta, \phi)$ for the three particular angles $\phi = 0^\circ$, 45° and 90° with respect to the reaction plane; here, the left inlet ($\phi = 0^\circ$) is the same as shown in Figure 2 in the middle column for U^{91+} ions. Again, the results from the electric dipole approximation are compared with those from a fully relativistic computation. As seen from Figure 3, the most pronounced effect of the higher multipoles arise for an electron emission in a plane, which is perpendicular to the photon polarization vector ($\phi = 90^\circ$). In such a — perpendicular — geometry of the experiment, the cross sections from the exact treatment show strong forward emission of the photoelectrons while the electric dipole approximation (26), in contrast, results in a completely isotropic emission, if seen as function of the polar angle θ .

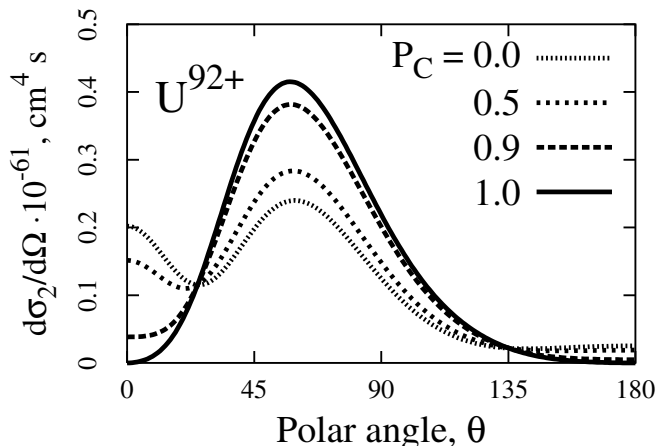


Figure 4. Angular distributions of the electrons emitted in the two-photon K -shell ionization of the hydrogen-like uranium U^{91+} by circular polarized light with different degrees of polarizations $P_C = 0, 0.5, 0.7,$ and 1 .

Until now, we considered the two-photon ionization of hydrogen-like ions by either *completely* polarized (linear: $P_L = 1$; circular $P_C = 1$) or unpolarized light ($P_L = P_C = 0$). In most experimental investigations on two- (and multi-) photon processes, however, the incident radiation is typically polarized with some given *degree of polarization* $0 \leq P_C, P_L \leq 1$. Apart from the *type* of the polarization of the incoming light, therefore, we shall study also how the angular distributions depend on the *degree* or polarization. Figure 4, for instance, displays the angular distribution from the K -shell ionization of hydrogen-like U^{91+} ions by means of circular polarized light with a degree of polarization $P_C = 0.0$ (unpolarized case), $0.5, 0.9$ and 1.0 . As seen from this figure, the probability for an electron emission increases at angles around $\theta = 60^\circ$ but decreases (towards zero) in forward and backward direction as the degree of polarization is increased. In particular the behaviour near $\theta = 0^\circ$ and $\theta = 180^\circ$ can be easily explained if we consider the conservation of momentum in the overall system. Since, for completely circular polarized light the (total) angular momentum of photons on the quantization axis (which is chosen along the photon momenta \mathbf{k}) becomes $\lambda_1 + \lambda_2 = \pm 2$, it obviously can not be compensated — in the final state — if the electron is emitted parallel (or antiparallel) to the incoming light, and hence its spin projection is $\mu_f = m_s = \pm 1/2$. For *unpolarized* light, in contrast, the photons may have different helicities and, hence, their angular momentum $\lambda_1 + \lambda_2 = \pm 0$ will be conserved under a forward and backward *non spin-flip* electron emission.

4. Summary

In this paper, the two-photon ionization of hydrogen-like ions has been studied in the framework of second-order perturbation theory *and* the relativistic description of the electron and photon fields. That is, exact Dirac bound and continuum wave functions

were applied for the description of the electron to reveal the importance of *relativity* on the angular distributions of the emitted electrons. Moreover, relativistic Coulomb–Green’s functions are used to perform the summation over the complete Dirac spectrum as needed in second-order perturbation theory.

To understand the angular distributions of the emitted photoelectron and, in particular, the influence of the polarization of the light on this emission, density matrix theory has been utilized to ‘combine’ the two-photon transition amplitudes in a proper way. Calculations are carried out for the K -shell ionization of the three (hydrogen-like) ions H, Xe⁵³⁺ and U⁹¹⁺. From the angular distribution of the electrons for different types (linear, circular, unpolarized) and degrees of polarization (i.e. in going from the completely polarized to unpolarized light), it is clearly seen that the angular emission depends much more sensitive on the contributions from higher multipoles than the total cross sections. Two rather pronounced effects, for example, concern the (asymmetrical) forward emission of the electrons as well as a significant change in the electron emission for linear polarized light, if the electrons are observed perpendicular to the reaction plane [cf. Figure 4]. Both effects are enhanced if the nuclear charge of the ions is increased.

An even stronger influence from the non-dipole terms (of the radiation field) is expected for the spin-polarization of the photoelectrons. Similar as in the present investigation, density matrix theory provides a very suitable tool for such *polarization* studies. A detailed analysis of the polarization of the photoelectrons, emitted in the two-photon ionization of hydrogen-like ions, is currently under work.

Appendix A. Photon spin density matrix

A *pure* (i.e. completely polarized) state of the photon can be characterized in terms of a polarization unit vector \mathbf{u} which always points perpendicular to the (asymptotic) photon momentum \mathbf{k} . Of course, this polarization vector, \mathbf{u} , can be rewritten by means of any *two* (linear independent) basis vectors such as the *circular polarization* vectors $\mathbf{u}_{\pm 1}$ which are (also) perpendicular to the wave vector \mathbf{k} and which, for \mathbf{u}_{+1} respective \mathbf{u}_{-1} , are associated with right- and left-circular polarized photons (Blum81). In such a basis, the unit vector for the *linear* polarization of the light can be written as

$$\mathbf{u}(\chi) = \frac{1}{\sqrt{2}} \left(e^{-i\chi} \mathbf{u}_{+1} + e^{i\chi} \mathbf{u}_{-1} \right), \quad (\text{A.1})$$

where χ is the angle between $\mathbf{u}(\chi)$ and the x - z plane.

While a description of the polarization of the light in terms of either the circular polarization vectors $\mathbf{u}_{\pm 1}$ or the linear polarization vector (A.1) is appropriate for completely polarized light, it is not sufficient to deal with an ensemble of photons which have different polarization. Such a — mixed — state of the light is then better described in terms of the spin–density matrix. Since the photon (with spin $S = 1$) has only two allowed spin (or helicity) states $|\mathbf{k}\lambda\rangle$, $\lambda = \pm 1$, the spin–density matrix of the photon

is a 2×2 matrix and, hence, can be parameterized by three (real) parameters:

$$\langle \mathbf{k}\lambda \mid \hat{\rho}_\gamma \mid \mathbf{k}\lambda' \rangle = \frac{1}{2} \begin{pmatrix} 1 + P_C & P_L e^{-2i\chi} \\ P_L e^{2i\chi} & 1 - P_C \end{pmatrix}, \quad (\text{A.2})$$

where $0 \leq P_L \leq 1$ and $-1 \leq P_C \leq 1$ denote the degree of linear and circular polarization, respectively. The angle χ , moreover, represents the direction of the maximal linear polarization of the light.

Of course, the choice of the parameters P_L , P_C and χ is not *unique* and many other — equivalent — sets of three real parameters could be applied to characterize the photon spin density matrix (A.2). In the analysis of experimental data, for instance, one often uses the three *Stokes* parameters to describe the polarization of radiation. The Stokes parameters can easily be expressed in terms of the (two) degrees of polarization, P_L and P_C , and the angle χ as:

$$P_1 = P_L \cos 2\chi, \quad P_2 = P_L \sin 2\chi, \quad P_3 = P_C. \quad (\text{A.3})$$

The use of the Stokes parameters leads to the familiar form of the spin density matrix (Balashov *et al* 2000)

$$\langle \mathbf{k}\lambda \mid \hat{\rho}_\gamma \mid \mathbf{k}\lambda' \rangle = \frac{1}{2} \begin{pmatrix} 1 + P_3 & P_1 - iP_2 \\ P_1 + iP_2 & 1 - P_3 \end{pmatrix}. \quad (\text{A.4})$$

References

- Antoine P, Essarroukh N–E, Jureta J, Urbain X and Brouillard F 1996 *J. Phys. B: At. Mol. Phys.* **29** 5367
- Arnous E, Klarsfeld S and Wane S, 1973 *Phys. Rev. A* **7** 1559
- Balashov V V, Grum–Grzhimailo A N and Kabachnik N M, 2000 *Polarization and Correlation Phenomena in Atomic Collisions* (New York: Kluwer Academic Plenum Publishers)
- Berestetskii V B, Lifshitz E M and Pitaevskii L P, 1971 *Relativistic Quantum Theory* (Oxford: Pergamon)
- Blum K, 1981 *Density Matrix Theory and Applications* (New York: Plenum)
- Eichler J and Meyerhof W, 1995 *Relativistic Atomic Collisions* (San Diego: Academic Press)
- Eichler J, Ichihara A and Shirai T, 1998 *Phys. Rev. A* **58** 2128
- Fano U and Racah G, 1959 *Irreducible Tensorial Sets* (New York: Academic Press)
- Fritzsche S, Inghoff T, Bastug T and Tomaselli M, 2001 *Comput. Phys. Commun.* **139** 314
- Goldman S P and Drake G W, 1981 *Phys. Rev. A* **24** 183
- Kornberg M A, Godunov A L, Ortiz S I, Ederer D L, McGuire J H and Young L 2002 *Journal of Synchrotron Radiation* **9** 298
- Koval P and Fritzsche S, 2003 *Comp. Phys. Comm.*
- Koval P, Fritzsche S and Surzhykov A, 2003 *J. Phys. B: At. Mol. Opt. Phys.* **36** 873
- Lambropoulos P, 1972 *Phys. Rev. Lett.* **28** 585
- Laplanche G, Durrieu A, Flank Y, Jaouen M and Rachman A, 1976 *J. Phys. B: At. Mol. Opt. Phys.* **9** 1263
- Laplanche G, Jaouen M and Rachman A, 1986 *J. Phys. B: At. Mol. Phys.* **19** 79
- Morse P and Feshbach H, 1953 *Methods of Theoretical Physics*, Vol. 1 (McGraw–Hill Inc., New York)
- Rose M E, 1957 *Elementary Theory of Angular Momentum* (Wiley, New York)
- Rottke H, Wolff B, Brickwedde M, Feldmann D and Welge K H, 1990 *Phys. Rev. Lett.* **64** 404

- Santos J P, Patte P, Parente F and Indelicato P, 2001 *Eur. J. Phys. D* **13** 27
- Surzhykov A, Fritzsche S and Stöhlker Th, 2002 *J. Phys. B: At. Mol. Opt. Phys.* **35** 3713
- Swainson R A and Drake G W F, 1991 *J. Phys. A: Math. Phys.* **24** 95
- Szymanowski C, Véniard V, Taïeb R and Maquet A, 1997 *Europhys. Lett.* **6** 391
- Wolff B, Rottke H, Feldmann and Welge K H, 1988 *Z. Phys. D* **10** 35
- Zernik W, 1964 *Phys. Rev.* **135** A51